

# Real-Time WAXD Detection of Mesophase Development during Quenching of Propene/Ethylene Copolymers

Dario Cavallo,<sup>†</sup> Giuseppe Portale,<sup>‡</sup> Luigi Balzano,<sup>§</sup> Fiorenza Azzurri,<sup>†</sup> Wim Bras,<sup>‡</sup> Gerrit W. Peters,<sup>§</sup> and Giovanni C. Alfonso<sup>\*,†</sup>

<sup>†</sup>Department of Chemistry and Industrial Chemistry, University of Genova, via Dodecaneso, 31-16146 Genova, Italy, <sup>‡</sup>Netherlands Organization for Scientific Research (NWO) DUBBLE CRG, European Synchrotron Radiation Facility, BP 220, F-38043, Grenoble Cedex, France, and <sup>§</sup>Department of Mechanical Engineering, Eindhoven University of Technology P.O. Box 513, 5600 MB Eindhoven, The Netherlands

Received September 30, 2010

Revised Manuscript Received November 19, 2010

**Mesomorphic Phase in Isotactic Polypropylene.** Synthetic semicrystalline polymers are generally characterized by a certain amount of disorder along the chains due to defects in the chemical constitution, in the configuration of neighboring repeating units, or in the conformation of a portion of molecule in the solid state.<sup>1</sup> When the polymer crystallizes under certain conditions, all these defects may hinder the packing of the chains, leading to a large amount of structural disorder. The definition of a crystalline unit cell becomes problematic when the degree of disorder is particularly high, and a structure with features intermediate between those of the crystalline and amorphous states is obtained.<sup>2</sup> This solid phase is usually referred to as “mesomorphic form” or “solid mesophase”, and it is rather frequently encountered in semicrystalline polymers.<sup>3,4</sup> Because of its industrial relevance, the mesophase of isotactic polypropylene (i-PP), which is easily obtained by quenching the molten polymer, has been extensively investigated.<sup>5–18</sup> Its structure is consistent both with the presence of small bundles of parallel chains in 3/1 helical conformation, with short-range lateral order,<sup>5</sup> and with a conformationally disordered glass, characterized by defects in the handedness of the helices.<sup>6</sup> The typical features of i-PP mesomorphic structure are reflected by its macroscopic properties, e.g., density,<sup>7</sup> intrinsic birefringence,<sup>8</sup> and elastic modulus,<sup>9</sup> which lay between those of the amorphous state and of the monoclinic structure. Formation and thermal stability of the i-PP mesophase have been investigated in detail.<sup>10–18</sup> The mesomorphic structure is metastable, and on heating between 40 and 80 °C, it undergoes a transformation into the thermodynamically stable crystalline  $\alpha$ -form.<sup>10–14</sup> The formation of the mesophase has been extensively studied by Piccarolo et al.<sup>15–18</sup> For the i-PP homopolymers, they demonstrated that a competition between formation of crystalline and mesomorphic order sets in on increasing cooling rate, and eventually, the latter prevails above ca. 100 °C/s. Associated with the development of the different structures, profound changes in the morphology have been reported. The typical cross-hatched lamellae of the  $\alpha$ -form spherulites are replaced in the semimesomorphic samples by small nodular morphologies lacking of any superstructure.<sup>15–18</sup>

**Kinetic Aspects of Mesophase Crystallization.** The kinetic aspects governing the development of the mesomorphic form are less understood, mainly because most of the information is obtained by ex-situ investigation of quenched samples. Formation of mesomorphic phases in semicrystalline polymers takes place only at very high undercooling, which are difficult to attain for a polymer exhibiting relatively high maximum crystallization rate as i-PP. One possibility to circumvent this problem is the cold crystallization of amorphous thin films ultraquenched below the glass transition. Isothermal crystallization of mesomorphic i-PP from the glass was studied by Myamoto et al.<sup>19</sup> by time-resolved SAXS/WAXD between –25 and –15 °C.<sup>20</sup> Confined crystallization of isotactic polypropylene has been studied on immiscible blends,<sup>21,22</sup> water dispersions,<sup>23,24</sup> and nanodroplets obtained by from surface dewetting.<sup>25</sup> In all cases, crystallization temperatures between ca. 20 and ca. 40 °C were reported. WAXD data<sup>22</sup> and AFM imaging<sup>25</sup> confirmed the development of the mesophase. Despite the scientific relevance of the above studies, the adopted crystallization conditions were very different from those practically encountered in polymer processing, i.e., fast cooling from the molten state, in which control of mesophase development is a key issue of technological relevance.<sup>26</sup>

So far, real-time measurements of mesomorphic structuring from the melt have only been performed by means of calorimetric techniques. In their pioneering work, Wunderlich et al.<sup>27</sup> detected mesophase formation between 60 and 0 °C upon cooling i-PP melts at ca. 70 °C/s. A meaningful step toward understanding of i-PP mesophase crystallization has recently been achieved thanks to ultrafast nanocalorimetry. De Santis et al.<sup>28,29</sup> have shown that for cooling rates above 150 °C/s an exothermic peak, which can be ascribed to mesophase formation, is detected between 40 and 20 °C, depending on the quenching conditions. Moreover, their isothermal crystallization experiments revealed that two bell-shaped curves, which intersect at ca. 45 °C, are required to describe the temperature dependence of the overall crystallization rate. The one at low temperature corresponds to the formation of the mesophase which, at room temperature, goes to completion in fractions of a second.

The development of the mesophase in i-PP based materials has recently been studied by us through the continuous cooling curves (CCC) diagrams, borrowed from metallurgy.<sup>30</sup> In these diagrams the acquisition of sample's temperature history during quenching reveals the time and temperature coordinates for the onset and completion of phase transitions. In the case of i-PP copolymers, this experimental approach has enabled us to distinguish between formation of the monoclinic  $\alpha$ -phase, occurring at higher temperature, and development of the mesophase, below 45–50 °C.

**Mesophase in i-PP-Based Random Copolymers.** Mechanical<sup>31,32</sup> and optical<sup>33</sup> properties of random copolymers of propene with  $\alpha$ -olefins can accurately be tailored through the control of chain microstructure. This possibility motivates the study of their crystallization behavior in processing-relevant cooling conditions involving the possible formation of the mesophase.<sup>30,34,35</sup> Mileva et al.<sup>34,35</sup> investigated the structure and morphology of random propene/1-butene copolymers quenched at different cooling rates. Their results show that the critical cooling rate required to obtain a semimesomorphic

\*To whom correspondence should be addressed. E-mail: Giovanni.Carlo.Alfonso@unige.it.

sample steadily decreases on increasing the concentration of counits. An analogous behavior was found by us for propene/ethylene copolymers.<sup>30</sup> This effect can easily be justified by considering the influence of copolymer composition on the crystallization kinetics of the monoclinic form. Indeed, it is well accepted that any type of counit acts as a defect hindering crystallization.<sup>36,37</sup> This results in a slowing down of the crystallization rate, a decrease of crystallinity, and a lowering of the melting temperatures on increasing comonomer content. While the issue is clear for what concerns the  $\alpha$ -form crystals, analogous understanding of the role of comonomeric units in the development of the mesophase is still lacking. To our knowledge, their effect on crystallization kinetics and their partitioning between amorphous and mesomorphic phase are still unexplored. In this paper, we address this specific topic by performing simultaneous in-situ thermal analysis<sup>30</sup> and real-time acquisition of WAXD patterns during fast cooling. Using synchrotron radiation and a state-of-the-art detector, the progressive development of semimesomorphic structure, which lasts less than 1 s, has been recorded for the first time. This approach opens new possibilities for real-time investigation of polymer crystallization at very high cooling rates and, in particular, of the role of molecular features on the formation of i-PP mesophase.

**Experimental Results.** The investigated materials are a commercial Ziegler–Natta isotactic polypropylene homopolymer and two random copolymers with 3.4 and 7.3 mol % of ethylene counits which were kindly provided by Borealis. Polymer films around 250–300  $\mu\text{m}$  thick, with a chromel–alumel  $\mu$ -thermocouple embedded in the midplane, were prepared according to the procedure earlier described.<sup>30</sup> The films were confined by 20  $\mu\text{m}$  thick aluminum foil tightly wrapped around them; this enabled efficient thermal exchange and low X-ray absorbance. Fast cooling experiments were performed in a home-built quenching device. The specimen is placed on a vertical holder where it can be heated up by a heating gun which fluxes hot air tangentially to the sample's wider surfaces. A control system allows to keep the sample at constant temperature. Quenching is performed by blowing compressed air nearly perpendicularly to both sides of the sample through two small hoses. The cooling rate can be varied either by regulating the flow rate of room temperature air, for cooling rates up to about 200  $^{\circ}\text{C}/\text{s}$ , or by varying the coolant temperature. The setup allows to place the sample with its wider surfaces perpendicular to the X-ray beam and to collect the diffracted signal in the transmission mode from a sampling volume less than 1 mm from the thermocouple head.

Wide-angle X-ray scattering (WAXS) experiments were performed at Beamline BM26B-DUBBLE at the ESRF using an X-ray radiation with wavelength of 1.269  $\text{\AA}$  focused on the sample with a spot size of approximately  $300 \times 400 \mu\text{m}$ . WAXS patterns were collected by a Pilatus 300 K-W pixel detector positioned at a sample-to-detector distance of 148 mm.  $2\theta$  scale calibration has been performed using the reflections of an high crystallinity  $\alpha$ -monoclinic i-PP sample. The use of the high frame rate Pilatus detector enabled us to collect 20 frames/s, with a remarkably good signal-to-noise ratio notwithstanding the small thickness of the sample and the short acquisition time of 47 ms. The readings of the instantaneous temperature were recorded from the  $\mu$ -thermocouple by a fast data-logger (HP 34970A), triggered by the detector in order to obtain perfect synchronization of temperature and WAXD signals. Samples were first melted at 210  $^{\circ}\text{C}$  and annealed at this temperature for 5 min before quenching at various cooling rates, from ca. 10 to ca. 200  $^{\circ}\text{C}/\text{s}$ .

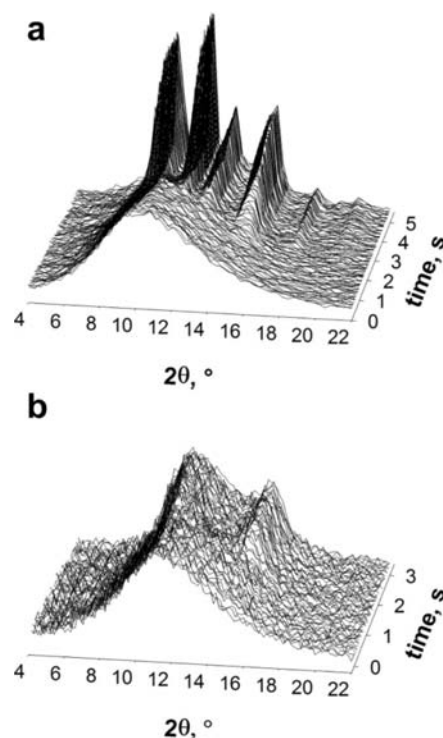


**Figure 1.** Examples of real-time WAXD patterns collected during the formation of monoclinic and mesomorphic phases. (a) i-PP homopolymer cooled at ca. 30  $^{\circ}\text{C}/\text{s}$ . (b) Propene/ethylene copolymer with 7.3 mol % of comonomer cooled at ca. 160  $^{\circ}\text{C}/\text{s}$ . For the sake of clarity, only one frame out of eight in (a) and out of four in (b) are shown.

Since the instantaneous cooling rate changes with sample's temperature, an average value, defined as the slope of the straight line connecting the origin of the temperature–time curve to the onset of the phase transition, has been considered.<sup>30</sup>

Typical examples of the evolution of the WAXD pattern during nonisothermal crystallization experiments leading to monoclinic and mesomorphic forms are shown in Figure 1. Figure 1a refers to development of the  $\alpha$ -phase in the i-PP homopolymer cooled at ca. 30  $^{\circ}\text{C}/\text{s}$ , while the series of patterns in Figure 1b pertains to the random copolymer with 7.3 mol % of ethylene counits solidified at an average cooling rate of ca. 160  $^{\circ}\text{C}/\text{s}$ . In both figures the WAXD signals collected in the time span in which the structuring takes place are shown. Time is counted from the instant the sample temperature reaches 195  $^{\circ}\text{C}$  during the fast cooling; this rescaling of the time axis is based on the consideration that 195  $^{\circ}\text{C}$  is a fair estimate of the equilibrium melting temperature of i-PP  $\alpha$ -crystals.

Detection of the onset of crystallization, as well as monitoring of the whole structuring process, is straightforward, even if the solidification occurs in a very narrow time window, i.e., less than 1 s for the mesophase. The quality of the series of time-resolved WAXD patterns is adequate to allow accurate evaluation of crystalline and mesomorphic phase fractions for any arbitrary time–temperature value. This estimation has been performed through frame by frame fitting of the smoothed amorphous halo obtained in the melt on the individual patterns. The percentage of ordered phase was then calculated by subtracting the contribution of the amorphous scattering from the total integrated diffracted intensity of the semicrystalline/semimesomorphic patterns. The accuracy of this analysis relies on the assumption of a simple biphasic system, i.e., a system in which either the

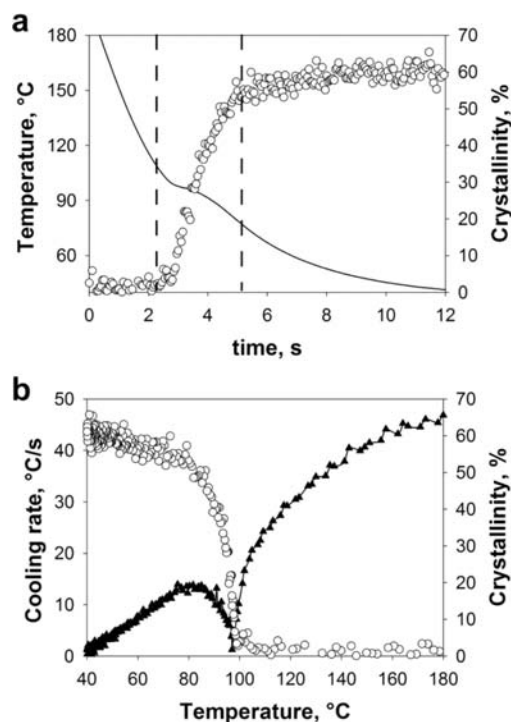


**Figure 2.** Comparison between thermal history and X-ray crystallinity for the i-PP homopolymer cooled at about 30 °C/s. (a) Instantaneous sample temperature and crystallinity (O) as a function of time. (b) Instantaneous cooling rate (▲) and crystallinity (O) as a function of temperature.

monoclinic or the mesomorphic phase is the only structured phase accompanying the amorphous one. This condition holds only for relatively low or relatively high cooling rates, while the two ordered structures coexists in comparable amounts for quenching conditions around the critical value of the cooling rate.<sup>15–18</sup> Indeed, the results of a previous structural analysis on the same polymers revealed that, for the propene/ethylene copolymers with 3.4 and 7.3 mol % of ethylene and the cooling conditions used in the present work, the  $\alpha$ -phase content is negligible, and the sample can safely be considered semimesomorphic.<sup>30</sup>

The development of structural order assessed by WAXD during the cooling experiments should be reflected also in the recorded cooling curves. We have previously shown that the release of the latent heat of crystallization results in a reduction of the cooling rate and thus in a deviation of the exponential temperature decay.<sup>30</sup> Simultaneously acquired temperature and WAXD data are directly compared in Figure 2 for the i-PP homopolymer cooled at about 30 °C/s, i.e., under conditions leading to formation of the  $\alpha$ -phase. Figure 2a unequivocally confirms the above observation. Crystallization indeed occurs in the region of the temperature plateau; in particular, it should be noted that the onset of the phase transition as revealed by WAXD and thermal signal perfectly coincide. This is further corroborated by Figure 2b, in which the temperature dependence of the instantaneous cooling rate is superposed to the X-ray crystallinity. The cooling rate deviates from the linear temperature dependence expected for the natural cooling and exhibits a relative minimum in correspondence with the maximum rate of crystallization revealed by WAXD. Substantial coincidence between WAXD and thermal signals was found also at higher cooling rates, when the developing structure is the mesomorphic phase rather than the monoclinic modification.

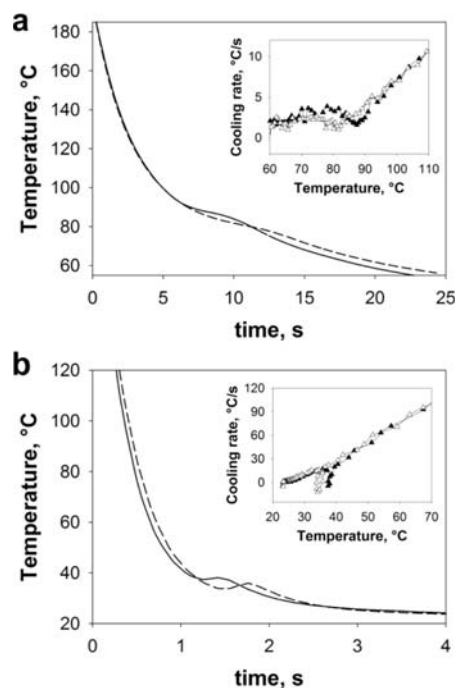


**Figure 3.** Thermal histories for propene/ethylene copolymers with 3.4 (solid line) and 7.3 mol % (dashed line) of comonomer, cooled at (a) 20 and (b) 160 °C/s. The insets show the temperature dependence of the instantaneous cooling rate for the copolymer with 3.4 (▲) and 7.3 mol % (Δ) of ethylene.

It can then be deduced that, in the adopted experimental conditions, i.e., sample size and cooling rates, temperature gradients across the sample thickness can be neglected. These results confirm our previous construction of CCC diagrams<sup>30</sup> and demonstrate that polymer crystallization at cooling rates relevant to processing can be studied in real time by synchrotron WAXD.

Structuring of i-PP homopolymer in the mesomorphic form requires rather high cooling rates, usually above ca. 100 °C/s; less severe conditions are needed for the development of the mesophase in random copolymers.<sup>30,32–35</sup> This makes easier to study the effect of comonomer concentration on nonisothermal crystallization of both types of ordered structures. The propene/ethylene copolymers with 3.4 and 7.3 mol % ethylene were cooled in identical conditions as shown by the thermal histories reported in Figure 3. The imposed cooling rates were approximately 20 °C/s for the development of the monoclinic crystals (Figure 3a) and 160 °C/s to obtain the mesomorphic form (Figure 3b). The insets show the coinciding cooling conditions for the different copolymers.

A closer look to Figure 3b reveals a slight self-heating, i.e., a negative cooling rate, due to the development of the mesophase at low temperatures. For both cooling conditions, on increasing the amount of ethylene counts, a decrease of the characteristic crystallization temperature, corresponding to the relative minimum in the cooling rate vs temperature plot, is evident. The shift is around 8 °C for the development of the  $\alpha$ -form and only about 3 °C when the mesophase is obtained.

The role of counts on crystallization kinetics is further demonstrated by Figure 4, in which the fraction of ordered phase is plotted as a function of time for the above-described cooling conditions.

In agreement with literature data, the  $\alpha$ -phase crystallinity is around 60% and decreases only slightly, down to 54%,



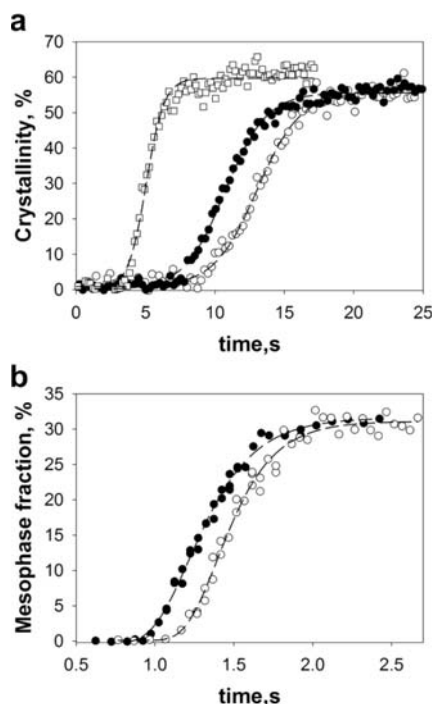


**Figure 4.** Time evolution of ordered structures during cooling at (a) 20 and (b) 160 °C/s for random propene/ethylene copolymers with 3.4 (●) and 7.3 (○) mol % of ethylene. Data for i-PP homopolymer (□) are added for comparison. Dashed lines represent sigmoidal fits to guide the eyes.

with increasing the content of ethylene counits.<sup>36,37</sup> The precise absolute degree of mesomorphic order is more difficult to obtain because it crucially depends on the evaluation procedure. Our estimate, around 30%, is in the range of previously reported values, i.e., 25–50%.<sup>13,16,30</sup> However, its knowledge is not relevant to discuss the kinetics of structure formation. The well-known hindering effect of constitutional defects on  $\alpha$ -phase crystallization kinetics<sup>36,37</sup> is clearly observed in Figure 4a. On increasing comonomer concentration from 0 to 7.3 mol %, the nonisothermal crystallization half-time increases by a factor of about 3 in association with the decrease of the crystallization temperature (Figure 3a). According to Alamo et al.<sup>37</sup> and De Rosa et al.,<sup>38</sup> this effect on crystallization kinetics can be ascribed to partial exclusion of ethylene units from the crystalline lattice. In fact, it has been demonstrated by solid state NMR that a fraction of various types of chain defects can partake in the formation of the crystalline phase. In the case of propene/ethylene random copolymers, De Rosa et al.<sup>38</sup> have shown that the crystal density lies in between those calculated assuming complete exclusion or total inclusion of the counits in the lattice. Alamo et al.<sup>37</sup> even succeeded in estimating the partitioning coefficient of the ethylene counits, i.e., the ratio between the concentration of ethylene in the crystalline regions to the sample-averaged concentration. It was found that ethylene counits are preferentially excluded, so that although they are present in the crystalline regions, their concentration is larger in the amorphous phase.

Figure 4b demonstrates that, by means of a very fast detector and a highly efficient quenching device, the process of mesomorphic ordering upon fast cooling from the melt can be monitored even if it lasts only few tenths of a second. Thus, one can investigate the impact of constitutional defects on the kinetics of mesomorphic crystallization. The experimental evidence shown in Figures 3b and 4b reveals that, also

for what concerns the mesophase formation, the structuring kinetics under identical cooling conditions (160 °C/s) slows down on increasing the concentration of ethylene counits. From these observations it can be inferred that, similarly to what happens during the formation of the  $\alpha$ -phase,<sup>36–38</sup> constitutional defects are preferentially excluded from the mesomorphic structure. In fact, ethylene counits cause a distortion of the 3/1 helical conformation of i-PP sequences, so that their inclusion in the monoclinic lattice is disfavored.<sup>38</sup> Since monoclinic and mesomorphic phase share the same chain conformation, we can argue that the same consideration holds also for the preferential exclusion of ethylene units from the mesophase, which results in a depression of ordering kinetics.

The results of our real-time detection of ordering processes under fast cooling conditions are consistent with and extend those obtained Mileva et al. by means of ultrafast nanocalorimetry.<sup>34</sup> They observed a decrease of the critical cooling rate required to obtain fully amorphous samples with increasing comonomer concentration in propene/ethylene and propene/1-butene copolymers. This implies that the maximum crystallization rate of the mesophase, besides that of the  $\alpha$ -phase,<sup>30,37</sup> decreases when the concentration of ethylene counits is increased. In other words, on increasing the content of counits, the CCC curve pertaining to development of the mesophase shifts toward longer times.

Interestingly, as we previously deduced from CCC diagrams,<sup>30</sup> the development of the  $\alpha$ -phase is more affected by the counits than that of the mesophase. Indeed, as shown in Figure 4, between the sample with 3.4 and 7.3 mol % of ethylene, a relative increase in the crystallization half-time of about 25% is observed for the formation of the monoclinic structure, while only ca. 15% increase is measured for the development of the mesophase. The different sensitivity of the structuring kinetics of the two ordered phases to copolymer composition is also reflected by the less marked shift of the crystallization temperature for the mesophase compared to that of the  $\alpha$ -phase, as it can be noticed in Figure 3. This less severe hindrance to the ordering process may be ascribed to the greater aptitude of this loosely packed and conformationally disordered polymorph<sup>3</sup> to host chain segments bearing constitutional defects. It is also worth considering that the hindering effect of the ethylene counits on crystallization kinetics mainly results from a remarkable decrease of the growth rate,<sup>37</sup> while the nucleation density is usually enhanced. Thus, the small size of the mesomorphic nodules makes this effect less dramatic.

**Conclusions.** Real-time structure development in i-PP and its copolymers with ethylene has been monitored, for the first time, by synchrotron WAXD during very fast cooling from the melt. We demonstrate that, by coupling online detection of the instantaneous sample's temperature with high-frequency acquisition of WAXD patterns, one can gain precise information on the rate at which ordered phases are formed in conditions relevant to actual processing. Thanks to the high time resolution attainable with novel X-ray detectors, the adopted approach has enabled us to probe the kinetics of mesophase structuring, which typically lasts a fraction of a second. Similarly to the  $\alpha$ -phase, the kinetics of mesophase development is appreciably delayed by the presence of random ethylene counits along the chain. However, the effect of constitutional defects appears to be slightly weaker for the mesomorphic phase than for the crystalline structure. This suggests that notwithstanding chain defects could be accommodated into the ordered structures, they are preferentially excluded also from the mesophase. The hindrance brought about by the smaller comonomeric units is apparently less

severe for the development of the mesomorphic nodules than for the growth of the  $\alpha$ -crystalline lamellae. This can be related to the lower free energy penalty for the inclusion of lattice defects in the already defective and looser mesomorphic structure and to the small size of the highly nucleated mesophase nodules which require lateral growth limited to only a few unit cells.

**Acknowledgment.** The fundamental contribution of Mr. Mario Traverso (University of Genova), who has designed and built the quenching device, is duly recognized. Authors are indebted to the personnel of beamline BM26/DUBBLE at the ESRF for assistance during the X-ray experiments. NWO (Netherland Organization for Scientific Research) is acknowledged for having granted the beamtime.

## References and Notes

- (1) Corradini, P. *The Stereochemistry of Macromolecules*; Ketley, A. D., Ed.; Marcel Dekker: New York, 1968; Vol. 3.
- (2) Corradini, P.; Guerra, G. *Adv. Polym. Sci.* **1992**, *100*, 183–217.
- (3) Auriemma, F.; De Rosa, C.; Corradini, P. *Adv. Polym. Sci.* **2005**, *181*, 1–74.
- (4) Androsch, R.; Di Lorenzo, M. L.; Schick, C.; Wunderlich, B. *Polymer* **2010**, *51*, 4639–4662.
- (5) Corradini, P.; Petraccone, V.; De Rosa, C.; Guerra, G. *Macromolecules* **1986**, *19*, 2699–2703.
- (6) Wunderlich, B.; Grebowicz, J. In *Liquid Crystal Polymers 2/3*; Platè, N., Ed.; Springer: Berlin, 1984; Vol. 60.
- (7) Vittoria, V. *J. Polym. Sci.* **1986**, *24*, 451–455.
- (8) Russo, R.; Vittoria, V. *J. Appl. Polym. Sci.* **1996**, *60*, 955–961.
- (9) Nitta, K.; Odaka, K. *Polymer* **2009**, *50*, 4080–4088.
- (10) Fichera, A.; Zannetti, R. *Makromol. Chem.* **1975**, *176*, 1885–1892.
- (11) O’Kane, W. J.; Young, R. J.; Ryan, A. J.; Bras, W.; Derbyshire, G. E.; Mant, G. R. *Polymer* **1994**, *35*, 1352–1358.
- (12) Wang, Z. G.; Hsiao, B. S.; Srinivas, S.; Brown, G. M.; Tsou, A. H.; Cheng, S. Z. D.; Stein, R. S. *Polymer* **2001**, *42*, 7561–7566.
- (13) Konishi, T.; Nishida, K.; Kanaya, T. *Macromolecules* **2006**, *39*, 8035–8040.
- (14) Androsch, R. *Macromolecules* **2008**, *41*, 433–435.
- (15) Piccarolo, S. *J. Macromol. Sci., Part B: Phys.* **1992**, *31*, 501–511.
- (16) Martorana, A.; Piccarolo, S.; Scichilone, F. *Macromol. Chem. Phys.* **1997**, *198*, 597–604.
- (17) Sondergaard, K.; Minà, P.; Piccarolo, S. *J. Macromol. Sci., Part B: Phys.* **1997**, *36*, 733–747.
- (18) Zia, Q.; Androsch, R.; Radusch, H. J.; Piccarolo, S. *Polymer* **2006**, *47*, 8163–8172.
- (19) Miyamoto, Y.; Fukao, K.; Yoshida, T.; Tsurutani, N.; Miyaji, H. *J. Phys. Soc. Jpn.* **2000**, *69*, 1735–1740.
- (20) Burns, J. R.; Turnbull, D. *J. Appl. Phys.* **1966**, *37*, 4021–4026.
- (21) Arnal, M. L.; Muller, A. J.; Maiti, P.; Hikosaka, M. *Macromol. Chem. Phys.* **2000**, *201*, 2493–2504.
- (22) Jin, Y.; Hiltner, A.; Baer, E.; Masirek, R.; Piorkowska, E.; Galesky, A. *J. Polym. Sci., Part B: Polym. Phys.* **2006**, *44*, 1795–1803.
- (23) Uriguen, J. I.; Bremer, L.; Mathot, V.; Groeninckx, G. *Polymer* **2004**, *45*, 5961–5968.
- (24) Ibarretxe, J.; Groeninckx, G.; Bremer, L.; Mathot, V. B. F. *Polymer* **2009**, *50*, 4584–4595.
- (25) Kailas, L.; Vasilev, C.; Audinot, J. N.; Migeon, H. N.; Hobbs, J. K. *Macromolecules* **2007**, *40*, 7223–7230.
- (26) Choi, C.; White, J. L. *Polym. Eng. Sci.* **2000**, *40*, 645–665.
- (27) Wu, Z. Q.; Dann, V. L.; Cheng, S. Z. D.; Wunderlich, B. *J. Therm. Anal.* **1988**, *34*, 105–114.
- (28) De Santis, F.; Adamovsky, S.; Titomanlio, G.; Schick, C. *Macromolecules* **2006**, *39*, 2562–2567.
- (29) De Santis, F.; Adamovsky, S.; Titomanlio, G.; Schick, C. *Macromolecules* **2007**, *40*, 9026–9031.
- (30) Cavallo, D.; Azzurri, F.; Floris, R.; Alfonso, G. C.; Balzano, L.; Peters, G. W. M. *Macromolecules* **2010**, *43*, 2890–2896.
- (31) Galahitner, M.; Jaaskelainen, P.; Ratajski, E.; Paulik, C.; Wolfschwenger, J.; Neissl, W. *J. Appl. Polym. Sci.* **2005**, *95*, 1073–1081.
- (32) Mileva, D.; Zia, Q.; Androsch, R. *Polym. Bull.* **2010**, *65*, 623–634.
- (33) Mileva, D.; Androsch, R.; Radusch, H. J. *Polym. Bull.* **2009**, *62*, 561–571.
- (34) Mileva, D.; Androsch, R.; Zhuravlev, E.; Schick, C. *Thermochim. Acta* **2009**, *492*, 67–72.
- (35) Mileva, D.; Zia, Q.; Androsch, R.; Radusch, H. J.; Piccarolo, S. *Polymer* **2009**, *50*, 5482–5489.
- (36) De Rosa, C.; Auriemma, F.; Ruiz de Ballesteros, O.; Resconi, L.; Camurati, I. *Chem. Mater.* **2007**, *19*, 5122–5130.
- (37) Jeon, K.; Palza, H.; Quijada, R.; Alamo, R. G. *Polymer* **2009**, *50*, 832–844.
- (38) De Rosa, C.; Auriemma, F.; Ruiz de Ballesteros, O.; Resconi, L.; Camurati, I. *Macromolecules* **2007**, *40*, 6600–6616.